

# Injectable and Thermosensitive Hydrogel Containing Liraglutide as a Long-Acting Antidiabetic System

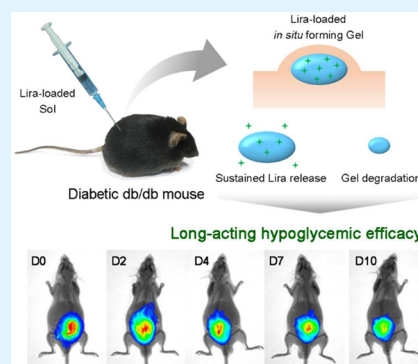
Yipei Chen, Jiabin Luan, Wenjia Shen, Kewen Lei, Lin Yu,\* and Jiandong Ding

State Key Laboratory of Molecular Engineering of Polymers, Department of Macromolecular Science, Fudan University, Shanghai 200433, China

## S Supporting Information

**ABSTRACT:** Diabetes, a global epidemic, has become a serious threat to public health. The present study is aimed at constructing an injectable thermosensitive PEG–polyester hydrogel formulation of liraglutide (Lira), a “smart” antidiabetic polypeptide, in the long-acting treatment of type 2 diabetes mellitus. A total of three thermosensitive poly( $\epsilon$ -caprolactone-*co*-glycolic acid)-poly(ethylene glycol)-poly( $\epsilon$ -caprolactone-*co*-glycolic acid) (PCGA–PEG–PCGA) triblock copolymers with similar molecular weights but different  $\epsilon$ -caprolactone-to-glycolide (CL-to-GA) ratios were synthesized. The polymer aqueous solutions exhibited free-flowing sols at room temperature and formed in situ hydrogels at body temperature. While the different bulk morphologies, stabilities of aqueous solutions, and the varying in vivo persistence time of hydrogels in ICR mice were found among the three copolymers, all of the Lira-loaded gel formulations exhibited a sustained drug release manner in vitro regardless of CL-to-GA ratios. The specimen with a powder form in the bulk state, a stable aqueous solution before heating, and an appropriate degradation rate in vivo was selected as the optimal carrier to evaluate the in vivo efficacy. A single injection of the optimal gel formulation showed a remarkable hypoglycemic efficacy up to 1 week in diabetic db/db mice. Furthermore, three successive administrations of this gel formulation within one month significantly lowered glycosylated hemoglobin and protected islets of db/db mice. As a result, a promising once-weekly delivery system of Lira was developed, which not only afforded long-term glycemic control but also significantly improved patient compliance.

**KEYWORDS:** liraglutide, type 2 diabetes mellitus, thermosensitive hydrogel, sustained drug release, in vivo degradation, hypoglycemic efficacy



## 1. INTRODUCTION

Diabetes mellitus, a chronic metabolic disease characterized by hyperglycemia and deterioration of pancreatic  $\beta$ -cell function, seriously challenges global public health. Although many antidiabetic agents such as insulin, sulphonylureas and metformin, can achieve well glycemic control, these drugs still suffer from various side effects and drawbacks like hypoglycemia, body weight gain and  $\beta$ -cell dysfunction. Recently, incretin-based therapies using glucagon-like peptide-1 (GLP-1) analogues or receptor agonists have drawn great attention.<sup>1–3</sup> GLP-1 is an incretin hormone of 30 amino acid residues that can stimulate insulin secretion in a glucose-dependent manner and thus control the blood glucose without the risk of hypoglycemia.<sup>4</sup> However, the rapid degradation of this hypoglycemic polypeptide via dipeptidyl peptidase IV (DPP-IV) results in a very short half-life (about 2 min) in human body, making it difficult for clinical application.<sup>5,6</sup> To overcome this problem, some GLP-1 analogues or receptor agonists have been developed.<sup>7,8</sup>

Liraglutide (Lira), a novel palmityl-acylated derivative of GLP-1, contains an Arg34Lys substitution and a 16 carbon fatty acid attaching to Lys26. These structural modifications prevent the degradation by DPP-IV and prolong the half-life of Lira to

about 13 h in plasma.<sup>9,10</sup> Lira maintains the positive physiological activities of GLP-1 including reducing blood glucose, improving  $\beta$ -cell mass and function, decreasing insulin resistance, delaying gastric emptying, and lowering body weight gain.<sup>11–13</sup> Particularly, insulin secretion stimulation in the glucose-dependent manner makes Lira with a minimal risk of hypoglycemia and less other side effects.<sup>14</sup>

The once-daily injection of Lira, also known as Victoza (Novo Nordisk), has been approved by the U.S. Food and Drug Administration (FDA) (2010) for glycemic control of adult patients with type 2 diabetes mellitus (T2DM). Its global sales have rapidly increased to \$2700 million in 2015, and it is a promising treatment option for T2DM. Nevertheless, the frequent administrations of Lira negatively affect patients' compliance. Therefore, a long-acting formulation of Lira with reduced frequency of administration is much desired and meaningful in clinical practice. In fact, it is challenging to achieve a formulation containing a high loading amount of Lira

**Received:** July 29, 2016

**Revised:** October 24, 2016

**Accepted:** October 27, 2016

**Published:** October 27, 2016

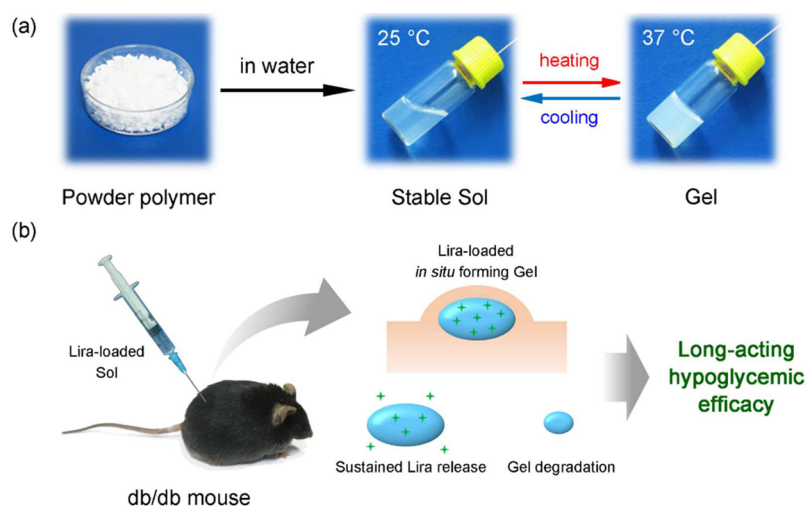


**Figure 1.** Schematic illustration of the long-acting antidiabetic formulation using injectable hydrogel. (a) The optimal thermosensitive polymers exhibited a powder form in bulk and thus was easy to handle. After dissolution in water, the polymer aqueous solution remained stable at room temperature and turned into an in situ hydrogel at body temperature. (b) Evaluation of long-acting hypoglycemic efficacy in diabetic db/db mice. The optimal polymer solution containing Lira formed an in situ drug depot after subcutaneous injection. Long-acting glucose-lowering effect was achieved by sustained release of drug, and then the residual hydrogel could be, in time, eliminated after the thorough release of Lira.

without significant degradation of the polypeptide drug and to keep a sustained release manner with neither significant burst effect at the initial stage nor evident incomplete release at the late stage. Meanwhile, diabetes patients need long-term treatment, and thus, the periodical administration of long-acting formulations is much-required. Correspondingly, the degradation rate of carriers should be taken into consideration when designing such a long-acting antidiabetic drug delivery system. Generally speaking, once the loaded drug is completely released from the previous formulation, the next formulation should be administrated to maintain the therapeutic efficacy. Thus, the residual carriers should be eliminated via degradation or absorption in the following some time to avoid their accumulation in the body.

Over the past decade, injectable polymeric hydrogels have been extensively investigated as promising carriers for sustained delivery of a variety of drugs due to their good biocompatibility, easy administration, and minimally invasive therapy.<sup>15–20</sup> In particular, injectable thermosensitive hydrogels exhibit free-flowing sols at room or low temperature yet turn into semisolid physical hydrogels with an increase of temperature.<sup>21–25</sup> Therefore, fragile therapeutic agents, such as protein, polypeptide or other small molecules, may be easily entrapped in the sol state at low temperature, and then the drug-loaded polymer solution spontaneously forms an in situ hydrogel at body temperature after injection into the body using a conventional syringe. Subsequently, the drugs could be released from the gel matrix in a sustained manner by drug diffusion or polymer degradation. To date, block copolymers of poly(ethylene glycol) (PEG)–polyester,<sup>26–28</sup> PEG–polypeptide,<sup>29,30</sup> and poly(phosphazene)s<sup>31,32</sup> have been reported as typically biodegradable and thermosensitive polymers undergoing a reversible sol–gel transition in water upon heating. Among them, thermosensitive polyester–PEG–polyester triblock copolymers are one of the most popular materials owing to the convenient synthesis of a one-pot reaction.<sup>26–28,33,34</sup> Also, their temperature-responsive gelation properties, polymer degradation behavior, and drug-release profiles can be easily modulated via molecular weight (MW) of each block, MW distribution of polymers, and types of polyester block.<sup>33–35</sup>

In the present study, we sought to develop a desired long-acting Lira delivery system using biodegradable and thermosensitive hydrogels made up of PEG–polyester copolymers as carriers. We synthesized three thermosensitive poly( $\epsilon$ -caprolactone-*co*-glycolic acid)-poly(ethylene glycol)-poly( $\epsilon$ -caprolactone-*co*-glycolic acid) (PCGA–PEG–PCGA) triblock copolymers with similar MWs but different  $\epsilon$ -caprolactone-to-glycolide (CL/GA) ratios. Their bulk properties and solution behavior in water were examined and compared. The in vitro release profiles of Lira were checked, and the in vivo degradation of the three hydrogels in ICR mice was also evaluated. Taking together the convenience of construction of Lira delivery system and the matching extent between the drug release profile and the degradation rate of carrier polymer, we confirmed the optimal Lira-loaded gel formulation and further detected its in vivo hypoglycemic efficacy upon a single subcutaneous injection into diabetic db/db mice, as illustrated in Figure 1. Finally, the glycosylated hemoglobin (HbA<sub>1c</sub>) and pancreatic islet morphology of db/db mice were also examined to assess the long-term glycemic control of animals after multiple subcutaneous injections of the optimal formulation.

## 2. MATERIALS AND METHODS

**2.1. Materials.** PEG with MW of 1500,  $\epsilon$ -caprolactone, and stannous 2-ethyl-hexanoate (stannous octoate, 95%) were purchased from Sigma-Aldrich. Glycolide was the product of Purac (Netherlands). Liraglutide was supplied by Chinese Peptide Co., Ltd. (Hangzhou, China). Cyanine5.5 *N*-hydroxysuccinimide ester (Cy5.5-NHS) was obtained from Lumiprobe. Glycosylated hemoglobin assay kit was supplied by Nanjing Jiancheng Bioengineering Institute (Jiangsu, China). All of the chemicals were used without further purification.

**2.2. Experimental Animals.** ICR mice (male, 30  $\pm$  2 g) were purchased from SLAC Laboratory Animal Co., Ltd. (Shanghai, China). Diabetic C57BLKS/J db/db mice (male, 6 weeks old) were obtained from Model Animal Research Center of Nanjing University (Jiangsu, China). All the animals were housed in cages under controlled temperature of 22–25 °C with a 12 h light–dark cycle. The mice had free access to standard laboratory chow diet and tap water. All procedures concerning laboratory animals were in accordance with the approved guidelines of the “Principles of Laboratory Animal Care”

(NIH publication no. 85–23, revised 1985) and were approved by the ethics evaluation board of Fudan University.

**2.3. Synthesis of Triblock Copolymers.** Polyester–PEG–polyester triblock copolymers were synthesized via a typical ring-opening polymerization of CL and GA using PEG 1500 as the macroinitiator and stannous octoate as the catalyst. The detailed synthetic procedure was described in our previous publications.<sup>36,37</sup> To synthesize the PCGA–PEG–PCGA triblock copolymer (P2), as an example, 15.0 g of PEG was first added into a dried three-necked flask and heated at 120 °C under vacuum for 3 h to eliminate the residual water absorbed to the polymer. Then, 3.6 g of GA, 31.4 g of CL, and 75 mg of stannous octoate was added in sequence, and the reaction mixtures were continuously stirred at 150 °C under an argon atmosphere for 12 h. After the reaction was finished, the flask was kept at 120 °C and connected to a vacuum line for 3 h to remove unreacted monomers. Finally, the resulting copolymer was washed three times using 80 °C deionized water and then freeze-dried to remove the residual water. The final product was collected and stored at –20 °C until use. The other two triblock copolymers with different polyester compositions were synthesized and purified via a similar procedure.

**2.4. <sup>1</sup>H NMR and Gel Permeation Chromatography.** <sup>1</sup>H NMR was performed in a 400 MHz <sup>1</sup>H NMR spectrometer (AVANCE III HD, Bruker) to determine the chemical compositions and structures of synthesized triblock copolymers. All spectra were recorded at room temperature using CDCl<sub>3</sub> (Sinopharm Chemical Reagent, China) as the solvent. A gel permeation chromatography (GPC) system (Agilent 1260) was used to analyze the MWs and MW distributions of copolymers. The eluent was tetrahydrofuran (TEDIA) with a flow rate of 1.0 mL/min at 35 °C. MWs were calculated by a series of polystyrene standards.

**2.5. Differential Scanning Calorimetry and X-ray Diffraction.** The thermal properties of copolymers were studied by a differential scanning calorimeter (Q2000, TA Instruments). A total of 5 mg of each sample was loaded into an aluminum pan. The samples were first heated to 80 °C and then held at this temperature for 5 min to eliminate the thermal history. Then, the cooling curves were recorded when the samples were cooled from 80 °C to –80 °C. After being kept at –80 °C for 5 min, the samples were heated to 80 °C again, and the heating curves were recorded as well. Both the cooling and the heating rates were 20 °C/min. The melting temperature ( $T_m$ ), crystallization temperature ( $T_c$ ), glass transition temperatures ( $T_g$ ), melting enthalpies ( $\Delta H_m$ ), and crystallization enthalpies ( $\Delta H_c$ ) were determined from the traces using the TA Universal Analysis software. X-ray diffraction (XRD) analysis was performed on a diffractometer (X'Pert PRO, PANalytical) equipped with a Cu K $\alpha$  radiation source. The copolymer samples were loaded in a glass lamella. The diffraction patterns of a scan range between 5° to 50° were recorded with a scanning rate of 5°/min at room temperature. The voltage was set at 40 kV, and the current was fixed at 40 mA.

**2.6. Bulk Morphologies and Aqueous Solution Stabilities of Copolymers.** The morphologies of the copolymers in the bulk state were observed, and their corresponding photographs were taken by a digital camera (Canon PowerShot S100 V). For the polymers with powder forms, their aqueous solutions were prepared by heating their polymer/water mixtures at 55–65 °C for a few minutes, followed by quenching in ice-water for no more than 30 min. As to the polymer exhibiting a sticky paste in the bulk state, the viscous sample was dissolved in water with continuous stirring over 1 day to obtain the polymer aqueous solution. To study the stabilities of the polymer aqueous solutions, the vials containing samples were stored in refrigerator at 4 °C overnight, and the corresponding photographs were recorded before and after storage.

**2.7. Sol–gel Transitions of Copolymer Aqueous Solutions.** The sol–gel transition temperature of copolymer aqueous solution was determined by the vial-inverting method<sup>38</sup> with a temperature increment of 1 °C per step. Briefly, 0.5 mL of polymeric solution in phosphate buffer saline (PBS, pH 7.4) was transferred into a 2 mL vial. The vials containing samples were then immersed in a water bath with the indicated temperature and equilibrated for 15 min. The sample was regarded as a gel if no visual flow was observed within 30 s after

inverting the vials. The experiments were performed in triplicate. The phase diagrams of copolymer solutions using temperature and concentration as coordinates were obtained after checking all the sol–gel–sol (suspension) transition temperatures.

**2.8. In Vivo Degradation of Polymer Hydrogels.** In vivo degradation behaviors of the three copolymer hydrogels were studied in ICR mice. A total of 36 mice were randomly divided into three groups ( $n = 12$  per group). The copolymer aqueous solutions with polymer concentration of 25 wt % were prepared by dissolving copolymers in PBS (pH 7.4) and sterilized by filtration through 0.22  $\mu$ m filters. Then, 0.2 mL of copolymer solution was subcutaneously injected into the backs of ICR mice to form an in situ gel. At predetermined time points, the mice were sacrificed by cervical dislocation, and the injection sites were carefully cut open. Photos of remaining gels in each group were taken by a digital camera (Canon PowerShot S100 V). The surrounding tissues containing the residual gels were also resected and fixed in 10% neutral buffered formalin and then embedded in paraffin. The tissues were sectioned at a 4  $\mu$ m thickness and stained with hematoxylin–eosin (HE). Histological observation was performed in a light microscope (ZEISS, Axiovert 200).

**2.9. In Vitro Drug Release.** Lira-loaded gel formulations were prepared by simply mixing drug with polymer aqueous solutions (PBS, 25 wt %) under a magnetic stirring at 4 °C. Subsequently, the copolymer solutions containing drug (2 mg/mL, 0.5 mL) were accurately transferred into the bottom of 10 mL test tubes (inner diameter 14 mm) and incubated at 37 °C to form physical hydrogels. Next, 5 mL of PBS (pH 7.4, 37 °C) was added as the release medium. The in vitro release systems were placed in a shaking water-bath at 37 °C with a fixed shaking rate of 50 rpm. At each interval of 1 day, the release medium was totally withdrawn and replaced by the same amount of fresh buffer. The experiments were performed in triplicate. The amount of released drug in medium was measured by a high-performance liquid chromatography (HPLC, Waters Separation Module e2695) using a C18 column (5  $\mu$ m particle, 150  $\times$  4.6 mm, Phenomenex). Mobile phase A was acetonitrile (Merck), and mobile phase B was water with 0.1% trifluoroacetic acid (J & K Chemical, China). A linear gradient with 48% mobile phase A and 52% mobile phase B to 56% A and 44% B was run in 20 min at a flow rate of 1.0 mL/min. The drug was detected by a UV detector (Waters UV–visible detector 2489) at 220 nm.

**2.10. In Vivo Imaging.** To monitor the in vivo Lira release, noninvasive, real-time fluorescence imaging was performed in ICR mice. Lira was labeled by Cy5.5 NHS at pH 8.4 with a molar ratio of 1:1. Unreacted dye was removed via dialysis, and Cy5.5-labeled Lira (Cy5.5-Lira) was obtained after lyophilization. Then, 0.2 mL of polymer aqueous solution (25 wt %) containing Cy5.5-Lira were subcutaneously injected into the backs of 10 ICR mice. The fluorescence of the whole body and isolated organs including liver, kidney, lung, spleen, and heart were monitored at 0, 2, 4, 7, and 10 days postinjection using an in vivo imaging system (In-Vivo Xtreme, Bruker) with an excitation wavelength of 690 nm and emission wavelength of 790 nm.

**2.11. Hypoglycemic Efficacy in Nonfasted db/db Mice.** The hypoglycemic efficacy of hydrogel formulation containing Lira was evaluated in nonfasted db/db mice. The polymer concentration of hydrogel was 25 wt %, and the drug-loading amount was 2 mg/mL. A total of 24 male db/db mice aged 8 weeks were randomly divided into three groups ( $n = 8$  per group). On the first day (defined as D0), the mice in the blank gel group received a single subcutaneous injection of polymeric hydrogel without drugs at a dosage of 7.5 mL/kg body weight, the Lira/Gel group received a single subcutaneous injection of Lira-loaded gel formulation (15 mg/7.5 mL/kg). While the group of Lira Solution was served as a positive control, the mice were administrated by once-daily subcutaneous injection of Lira solution at a one-tenth dosage of the gel formulation (1.5 mg/7.5 mL/kg), and the total dosage of Lira solution was equal to that of Lira-loaded gel formulation during the 10 day experimental period. All of the mice were kept under nonfasted conditions with free access to food and water until the end of experiment. At 0, 4, 8, 12, 24, 48, 72, 96, 120,

Table 1. Composition Parameters of the Copolymers Synthesized in This Study

sample	composition	$M_n^a$	CL/GA (mol/mol) <sup>a</sup>	$M_n^b$	$(M_w/M_n)^b$
P1	PCL-PEG-PCL	1900–1500–1900	—	8190	1.38
P2	PCGA-PEG-PCGA	1845–1500–1845	5:1	7640	1.35
P3	PCGA-PEG-PCGA	1850–1500–1850	1:1	7230	1.28

<sup>a</sup>The  $M_n$  of the central block PEG was provided by Sigma-Aldrich. The  $M_n$  of polyester block and molar ratios of CL and GA units were calculated by <sup>1</sup>H NMR. <sup>b</sup>Measured by GPC, relative to polystyrene standards.

144, 168, 192, 216, and 240 h post-administration, a drop of blood was obtained from the tail vein of each mouse to measure the blood glucose level using a blood glucose meter (AccuCheck Active, Roche Diagnostics). Subsequently, on day 10 and day 20 after the first administration of gel formulation, the mice in the blank gel and Lira/Gel groups received twice injections of blank gel or Lira-loaded gel formulation, respectively. Correspondingly, the mice in the group of Lira Solution received a once-daily injection of Lira solution in the next 20 days. In addition, body weights of all animals were measured every day at 9 a.m.

On day 30, blood samples of all the mice were collected from the eyes. HbA<sub>1c</sub> levels in plasma were determined by a glycosylated hemoglobin assay kit.

**2.12. Histological and Immunohistochemistry Studies.** After the animals were sacrificed by euthanasia, the pancreases of db/db mice were isolated and then fixed in 10% neutral buffered formalin. After being embedded in paraffin, the pancreatic tissues were sectioned by 4  $\mu$ m and stained with HE for histological observation. Insulin immunohistochemistry was also performed to measure the proliferation of  $\beta$  cells in the pancreas.<sup>39,40</sup> The tissues embedded in paraffin were sectioned by 4  $\mu$ m. Endogenous peroxidase blocking process was performed after a 10 min pretreatment at room temperature. First, paraffin sections were treated with rabbit anti-insulin antibody (Cell Signaling Technology, Inc.) diluted at a ratio of 1/800 as the primary antibody at 4 °C overnight and then washed three times using PBS. Next, biotin-labeled secondary antibody (Maixin Biotech, China) was added, and the samples were incubated for 10 min at room temperature and then washed three times using PBS. Finally, sections were stained with 3,3'-diaminobenzidine (DAB, Maixin Biotech, China) and counter-stained with hematoxylin. Photomicrographs of all the slices were captured by a light microscope (ZEISS, Axiovert 200).

**2.13. Statistical Analysis.** All of the results were expressed as mean  $\pm$  standard deviation (SD). Comparisons between groups were analyzed by Student *t* tests, and a *p* value of less than 0.05 was considered as a significant difference, unless otherwise indicated.

### 3. RESULTS

**3.1. Synthesis and Characterization of Triblock Copolymers.** The triblock copolymers were synthesized via ring-opening polymerization of CL and GA in the presence of PEG, catalyzed by stannous octoate. The obtained samples were characterized by <sup>1</sup>H NMR and GPC. According to the previous protocols,<sup>36,37</sup> the number-average MWs ( $M_n$ ) and CL-to-GA ratios of the copolymers were determined via <sup>1</sup>H NMR spectra, as shown in Figure S1. Herein, PCL-PEG-PCL triblock copolymer without GA segments was named as P1, while PCGA-PEG-PCGA triblock copolymers with CL-to-GA ratios of 5:1 and 1:1 were referred to as P2 and P3 samples, respectively. Their weight-average MWs ( $M_w$ ) and MW distributions were further confirmed by GPC analysis, and a unimodal pattern with polydispersity index ( $M_w/M_n$ ) of less than 1.40 was observed in the GPC traces for all the samples, as presented in Figure S2, suggesting that the polymerization was successfully performed and the desired products were synthesized. The detailed compositions of copolymers in this study are summarized in Table 1.

**3.2. Thermal Properties and Aqueous Solution Stabilities of Copolymers.** The differential scanning calorimetry (DSC) thermograms of copolymers with varying CL-to-GA ratios are shown in Figure 2a. Crystalline P1

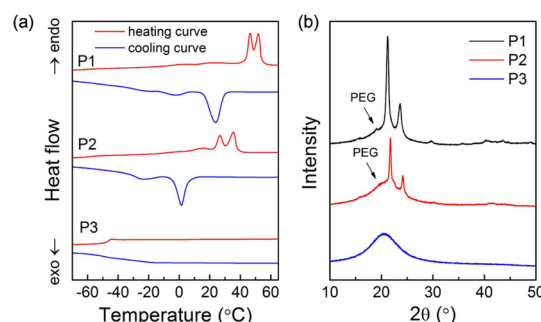


**Figure 2.** Thermal properties of the copolymers indicated in Table 1. (a) DSC thermograms. The heating and cooling rate was 20 °C/min. (b) XRD patterns.

copolymer presented a bimodal endothermic peak at 46 and 52 °C in the heating curve, which was assigned to the melting of PCL constituent followed by the melting of recrystallized PCL domain.<sup>41,42</sup> Meanwhile, a weak melting peak at 24 °C in the heating curve was also observed, which were attributed to the PEG segment. The cooling process presented two exothermic peaks at 4 and 24 °C, which came from the crystallization of PEG and PCL, respectively. These findings were well coincided with similar PCL-PEG-PCL copolymers reported elsewhere.<sup>41,42</sup> The incorporation of GA segment into PCL blocks greatly hindered the crystallization of PCL. Consequently, shifts of melting and crystallization peaks to lower temperature were observed in the P2 system. For example, the double melting peak of PCL segment shifted to 26 and 35 °C in the heating curve. Also, the crystallization peak of PCL was located at 2 °C, while that of PEG appeared at −23 °C in the cooling curve. In the case of P3 copolymer, neither melting peak nor crystallization peak was detected in both the heating and cooling cycles, suggesting the amorphous state of this copolymer. Nevertheless, a remarkable glass transition at −47 °C was observed during the heating process of P3. The detailed DSC data including  $T_m$ ,  $T_c$ ,  $\Delta H_m$ ,  $\Delta H_c$ , and  $T_g$  are summarized in Table S1. We also applied PEG1500 as a control. From the DSC data of PEG1500, P1, and P2, we further found that the introduction of PCL segments resulted in the decrease of  $T_m$  and  $T_c$  of PEG in P1 and P2 systems. The reason is that earlier crystallization of the PCL segment freezes the whole structure and hinders the crystallization process of PEG block.<sup>41</sup>

The XRD measurements were also performed to confirm the crystalline behavior of the three copolymers. As shown in Figure 2b, the XRD pattern of P1 copolymer exhibited two strong diffraction peaks at 21.4° and 23.8°, which came from the crystallization of the PCL segments. Meanwhile, a weak diffraction peak at 19.4° was also observed, which was

attributed to the crystallization of the PEG domain.<sup>43</sup> While P2 copolymer presented a similar pattern of P1, the peak intensities were lower than those of P1, reflecting the decrease of crystallization due to the incorporation of GA units. No crystallization peak was found in P3 system, demonstrating its amorphous state. These features are well consistent with the DSC results.

The morphologies of the three copolymers in the bulk state are presented in Figure 3a. Both P1 and P2 specimens exhibited

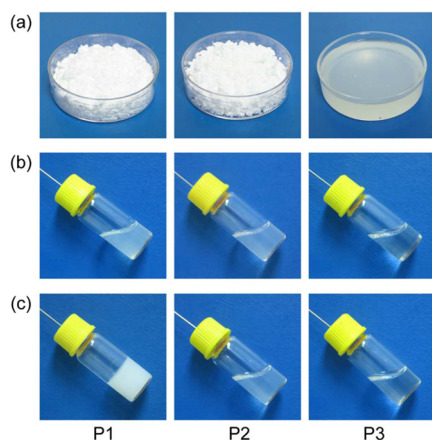


**Figure 3.** Photographs of the indicated copolymers in bulk and their aqueous solutions. (a) Powder states of P1 and P2 vs sticky paste of P3 at room temperature. (b) The aqueous solutions of the three copolymers after dissolution in PBS (pH 7.4, 25 wt %). (c) Unexpected gelation of P1 solution vs stable sol states of P2 and P3 solutions after being stored at 4 °C overnight. P2 was the only copolymer exhibited a powder state in bulk and was kept a stable sol state in water among the three copolymers.

powder forms, enabling convenient preparation of their aqueous solutions. In contrast, P3 just showed a sticky paste state in bulk, which was difficult to weigh, transfer, and handle, and continuous stirring over 1 day was required to dissolve the viscous polymers in water. Figure 3b displays their aqueous solutions with polymer concentration of 25 wt %. After being stored in a refrigerator at 4 °C overnight, the copolymer aqueous solution of P1 spontaneously formed an opaque gel because of crystallization, as presented in Figure 3c. In comparison, P2 and P3 solutions remained the free-flow sol states, even after several days of storage.

**3.3. Sol–Gel Transitions of Copolymers in Water.** The three specimens were dissolved in water at ambient temperature and formed in situ hydrogels as the temperature increased. Figure 4 shows their phase diagrams in PBS (pH 7.4). P1 system exhibited a smaller critical gelation concentration (CGC) (about 6 wt %) compared with those of P2 and P3 (about 12 wt %). The formation of a percolation micellar network via micellar aggregation was responsible for the temperature-induced gelation of polyester–PEG–polyester copolymers in water.<sup>35</sup> The micellar reorganization and aggregation of the PCGA–PEG–PCGA system with the incorporation of GA segment may become difficult compared with the PCL–PEG–PCL system. As a result, a higher CGC was needed for the PCGA–PEG–PCGA hydrogel. In contrast, the sol–gel transition temperatures of P1 copolymer solutions were higher than those of P2 and P3. For example, the sol–gel transition temperatures of P1, P2, and P3 copolymer solutions at the same concentration of 25 wt % were 36, 30, and 28 °C,

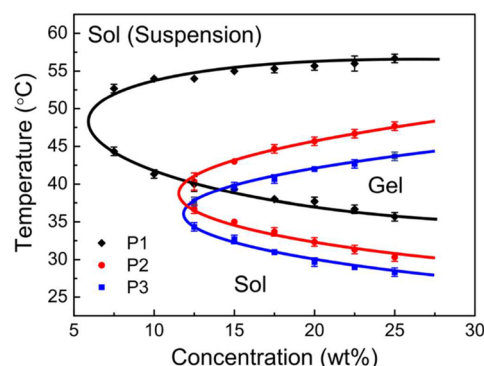


**Figure 4.** Phase diagrams of the indicated samples in PBS (pH 7.4). The sol–gel transition temperatures were determined by the vial-inverting method.  $n = 3$  for each sample.

respectively. This feature indicates that the sol–gel transitions of polyester–PEG–polyester systems may be influenced by many factors, such as molecular structure, hydrophobicity and crystallization tendency of polyester block, etc. The intrinsic reasons for differences in sol–gel transition temperatures among the three systems with different polyester compositions are still open, and further studies are required. Luckily, the gel regions covered body temperature (37 °C) for all the three copolymer/water systems, indicating that these injectable thermosensitive hydrogels with proper concentrations are suitable for biomedical applications.

**3.4. In Vivo Degradation of Hydrogels.** In vivo degradation of all the three thermosensitive hydrogels was examined after subcutaneous injection into ICR mice. Some representative images are shown in Figure 5. The copolymer aqueous solutions spontaneously transformed into in situ physical hydrogels within half a minute after injection. The opaque gels with spherical morphology were observed at day 1 postinjection, and the size of the three gels gradually decreased following the hydrolysis of polyester segments. P1 gel maintained its integrity over 56 days, indicating the very slow degradation rate; P2 gel was eliminated from the mice for no more than 4 weeks; P3 gel exhibited the fastest degradation rate and disappeared within 3 weeks. These results indicate that the in vivo degradation rate of hydrogels may be modulated by the GA contents in the copolymers.

The inflammatory response of tissues surrounded the hydrogels at different time points was also evaluated by histological observation. Figure 6 shows the optical micrographs of HE-stained slices of surrounding connective and muscular tissues after subcutaneous injection of P2 hydrogel into ICR mice. Similar to other thermosensitive PEG–polyester hydrogels,<sup>44–46</sup> P2 hydrogel induced an acute inflammation response in the first week and a number of inflammatory cells such as lymphocytes and macrophage infused into the surrounding tissue (Figure 6b,c). As the time went on, the acute inflammation gradually turned into a mild chronic inflammation, as evidenced by significant reduction of inflammatory cells at 3 weeks postinjection (Figure 6e), and almost no inflammatory cell was observed after the complete degradation of hydrogel at day 28 (Figure 6f), suggesting that the affected region was restored to the normal state. Besides, no sign of tissue necrosis, hemorrhaging, hyperemia, or edema was observed at the administration site during the whole period of examination. These features demonstrated that these PEG–

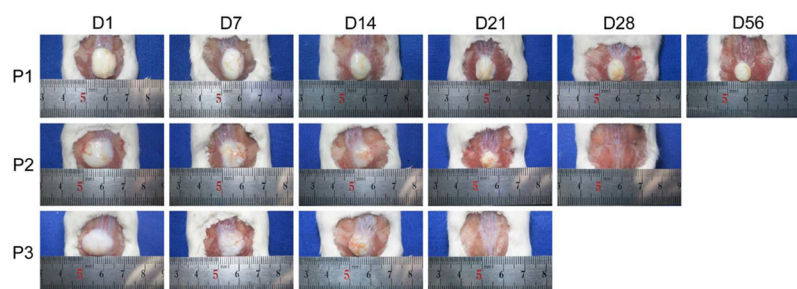


**Figure 5.** In vivo degradation behavior of the indicated thermosensitive hydrogels in ICR mice. The photographs were taken at predetermined time after subcutaneous injections of the indicated gels. “D” denotes “day”.

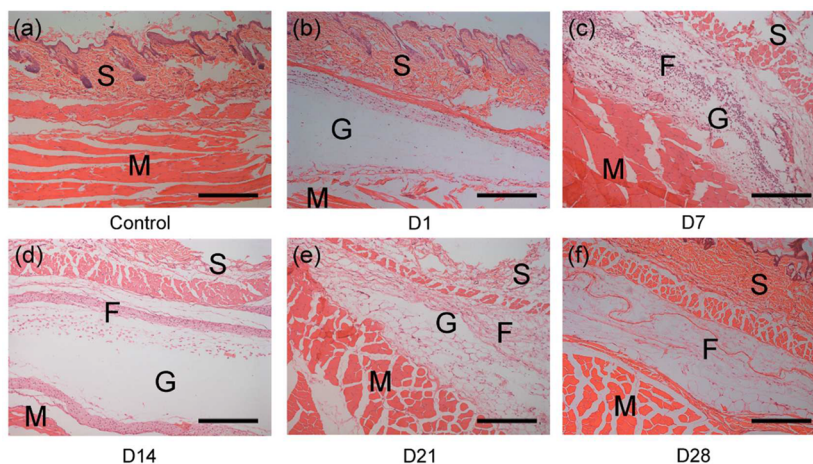


**Figure 6.** Optical micrographs of HE-stained slices of surrounding tissues: (a) normal control and at (b) 1 day, (c) 7 days, (d) 14 days, (e) 21 days, and (f) 28 days after subcutaneous injection of P2 hydrogel (25 wt %) into ICR mice. S: skin tissue; M: muscle tissue; F: fibrous connective tissue; G: hydrogel. Scale bar: 500  $\mu\text{m}$ .

polyester hydrogels have acceptable biocompatibility as implantable biomaterials.

**3.5. In Vitro Release of Lira.** In vitro release profiles of Lira from the hydrogels were investigated, and the results are presented in Figure 7. All the three Lira-loaded gel systems exhibited a similar sustained release manner up to 10 days, and the cumulative release amounts reached about 70–80%. The release data were further fitted via the Higuchi equation,  $Q = kt^{1/2}$  ( $Q < 0.6$ ), where  $Q$  is the cumulative release amount,  $t$  is release time, and  $k$  is a constant.<sup>47</sup> All of the release data well matched with the Higuchi equation with  $R^2 > 0.99$  (Table S2),

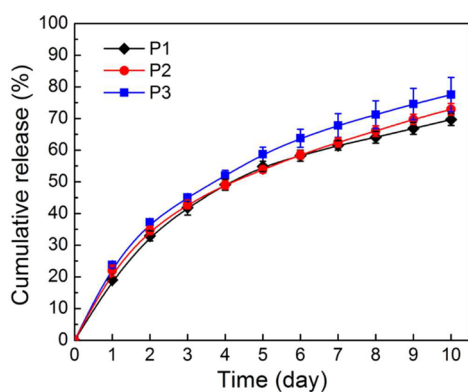


**Figure 7.** In vitro release profiles of Lira from the indicated hydrogels. Copolymer concentration was 25 wt %, and the drug-loading amount was 2 mg/mL. Data are presented as mean  $\pm$  SD  $n = 3$  for each group.

indicating that the diffusion-controlled mechanism governed the release of drug from these hydrogel matrices.

**3.6. In Vivo Imaging of Lira from the P2 Hydrogel System.** In vivo fluorescence imaging of Lira was carried out to monitor the release behavior of Lira from hydrogel in ICR mice. Considering both the convenience of administration and the matched degradation rate, we selected Lira-loaded P2 hydrogel formulation as the optimal drug delivery system. The drug was first labeled by Cy5.5, and then the P2 polymer solution containing Cy5.5-Lira was subcutaneously injected into the backs of ICR mice. As shown in Figure 8a, the fluorescence of Cy5.5-Lira was clearly observed at injection site, and the intensity gradually diminished within the next 10 days, reflecting the sustained release of drug out of the gel matrix. As is well-known, the widely distributed endogenous enzymes, like DPP-IV, in multiple organs and tissues are involved in the in vivo degradation of Lira after subcutaneous injection.<sup>4,48</sup> Hence, ex vivo imaging of the major organs was also performed to track the distribution of degradation products of Lira. The fluorescence was observed in both livers and kidneys, as shown in Figure 8b, which was accounted for the degradation segments of released Cy5.5-Lira, and they were further eliminated by glomerular filtration.

**3.7. In Vivo Hypoglycemic Efficacy.** Hypoglycemic efficacy of Lira-loaded P2 gel formulation was evaluated in nonfasted diabetic db/db mice. The mice receiving a single injection of blank gel without drug maintained high blood-glucose levels during the whole experimental period. According to Figure 9, glucose-lowering effects were achieved by once-

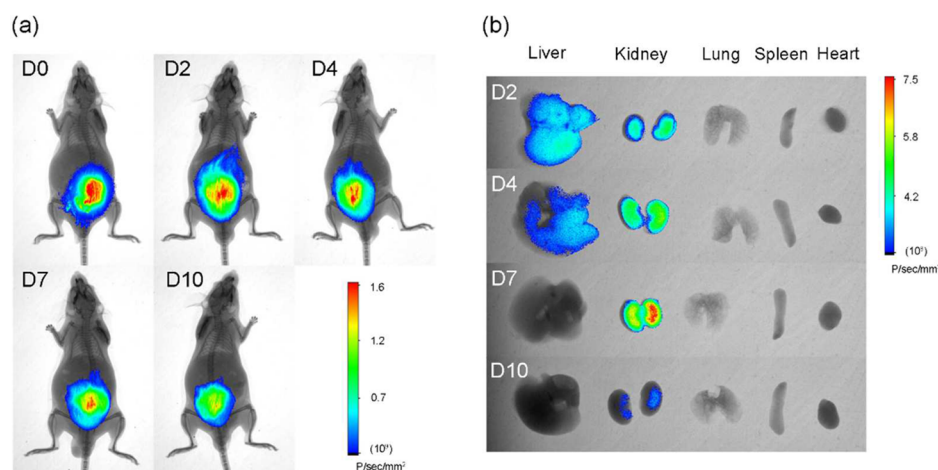


**Figure 8.** Fluorescent imaging of Lira released from hydrogel. (a) Monitoring of Cy5.5-Lira in P2 gel at the different time points after subcutaneous injection in ICR mice. (b) Ex vivo imaging of degradation products of released Cy5.5-Lira in major organs. The livers, kidneys, lungs, spleens, and hearts were isolated from mice at the different time points after subcutaneous injections. “D” denotes “day”.

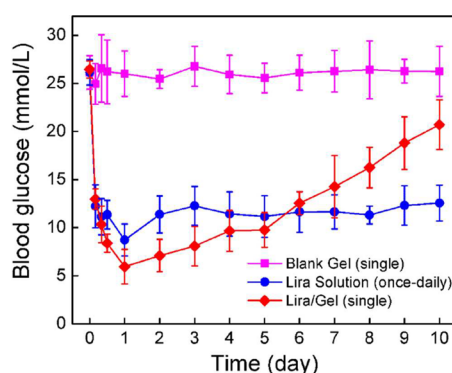


**Figure 9.** Blood glucose levels of nonfasted db/db mice after administration of the different formulations. Data are presented as mean  $\pm$  SD  $n = 8$  for each group.

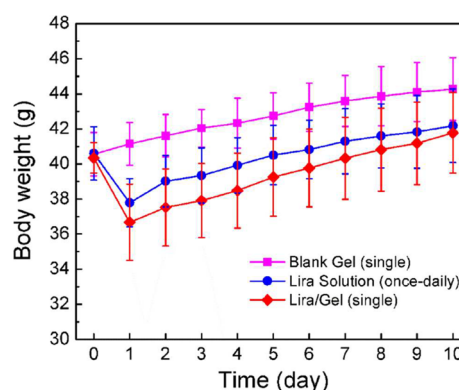


**Figure 10.** Body weights of db/db mice after the indicated treatments. Data are presented as mean  $\pm$  SD  $n = 8$  for each group.

daily administration of Lira solution in mice. The blood glucose levels of mice were also effectively lowered after a single subcutaneous administration of the Lira-loaded gel formulation. Its hypoglycemic efficacy was not significantly different from that achieved by once-daily injection of Lira solution in the first 7 days. Meanwhile, a lower blood glucose level was observed even at day 10 postinjection compared with that of the blank gel group.

The mice were also weighed everyday morning. As shown in Figure 10, the body weights of mice in the blank gel group steadily increased over time-scale. In contrast, the body weights of mice greatly decreased after the administration of Lira solution or Lira-loaded gel formulation. Compared with the group of Lira solution, a relatively more-remarkable reduction of body weights was observed in the group of Lira/Gel formulation during the whole experimental period, indicating that the more-steady blood drug concentration achieved by the sustained release of Lira provided a higher efficiency of gastric emptying delay and appetite reduction.

**3.8. Long-Term Glycemic Control.** To evaluate the long-term glycemic control of the Lira-loaded gel formulation in model animals, two subsequent administrations of Lira-loaded gel formulation were carried out on day 10 and day 20 after the first treatment. After 1 month, the mice were sacrificed, and their blood was collected from their eyes. The HbA<sub>1c</sub> levels in

the plasma was detected by a glycosylated hemoglobin assay kit. HbA<sub>1c</sub> comes from irreversible glycation of hemoglobin and reflects a total condition of pilot of the plasma glucose over a long time. Hence, HbA<sub>1c</sub> is acknowledged as a reliable index for the long-term glycemic control.<sup>49</sup> In this study, compared with levels in the blank gel group, a significant decrease of HbA<sub>1c</sub> was observed in those mice who received the treatment of Lira solution or Lira-loaded gel formulation (Figure 11). Meanwhile, there was no significant difference of HbA<sub>1c</sub> between the Lira solution and Lira/Gel formulation groups, indicating that the efficacy of the Lira-loaded gel formulation is equal to that of a once-daily injection of Lira solution in long-term glycemic control.

**3.9. Histological and Immunohistochemistry Examination.** To examine the effects of the Lira-loaded gel formulation on the islet morphology and  $\beta$ -cell function, HE staining and immunocytochemical staining of pancreatic tissues isolated from animals were performed. As shown in Figure 12a, the islet of mice in the blank gel group exhibited boundary definition loss and degeneration, whereas the morphology of islet of mice receiving the treatment with Lira solution or with the Lira-loaded gel formulation was normal, which presented a round or elliptical shape with a distinct boundary and tight organization between islet cells, suggesting the sustained proliferation of  $\beta$  cells following administration of Lira. In addition, the mice pancreatic tissues were immunostained for

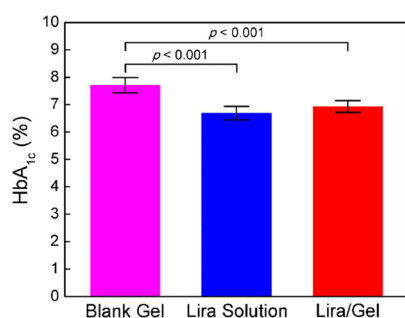


**Figure 11.** HbA<sub>1c</sub> levels in plasma of db/db mice after the indicated treatments for 30 days. Lira solution was administrated via once-daily subcutaneous injection throughout the whole experimental period. The Lira-loaded gel formulation was subcutaneously injected three times on day 0, 10, and 20. Data are presented as mean ± SD  $n = 8$  for each group.

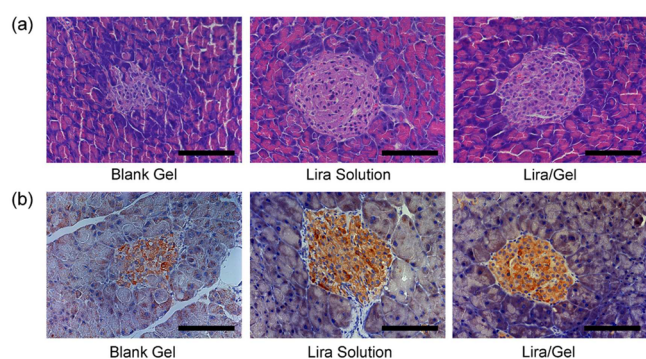


**Figure 12.** Representative images of histological sections of pancreatic islet isolated from db/db mice upon indicated treatments for 30 days. (a) HE-stained. (b) Insulin-immunostained. Scale bar: 100  $\mu$ m.

insulin to detect  $\beta$  cells. Representative section images are presented in Figure 12b. The insulin-positive signals with brown color of DAB means the insulin secretion in islets and thus directly reflect the existence of islet  $\beta$  cells.<sup>39,40</sup> The DAB-stained intensity in the blank gel group was weak, indicating the loss of insulin-producing  $\beta$  cells in the pancreas islet. In contrast, the staining intensities in both the Lira solution and the Lira/Gel groups were greatly higher than that in the blank gel group, implying the prevention of  $\beta$  cells loss in pancreas islet after the treatment of Lira. Combining with the results of HE staining and insulin immunostaining, we confirmed that both the Lira-loaded gel formulation and Lira solution can protect the pancreases and improve the pancreatic function of db/db mice.

#### 4. DISCUSSION

Lira, a fatty acid derivative of GLP-1, is designed for once-daily injection in treatment of T2DM because of its half-life of 13 h.<sup>9,10</sup> For the reduction of injection frequency and improvement of patients' compliance, developing long-acting Lira formulations is very meaningful and important in clinics but challenging in pharmaceuticals and material science. It is well-known that high-dose administration of antidiabetic agents such as insulin may cause severe hypoglycemic shock and even death. Unlike insulin, Lira is capable of stimulating insulin secretion in a blood-glucose-dependent manner, and this feature makes it suitable for sustained delivery to achieve long-acting glycemic control without the hypoglycemic risk.

In the past decade, injectable thermosensitive PEG–polyester copolymers hydrogels have been extensively suggested as promising carriers for the delivery of various protein and polypeptide drugs in the treatment of different diseases.<sup>45,47,50,51</sup> In this study, a series of thermosensitive PCGA–PEG–PCGA triblock copolymers with different CL-to-GA ratios were designed and synthesized and then utilized to encapsulate and deliver Lira. To achieve an ideal delivery system of Lira, the following three points should be taken into account and satisfied: (1) it is easy to construct and handle such a delivery system; (2) the delivery system can realize a sustained drug release; (3) the carrier polymer has an appropriate degradation rate and thus matches with the release period of drugs to avoid the accumulation of polymer residues after repeated administrations.

#### Easy-to-Handle Carrier Polymers and Proper in Vivo Persistence Time of Hydrogels.

Among the thermosensitive polymers synthesized by us, PCL–PEG–PCL triblock copolymers (P1) presented a powder form in bulk. However, its aqueous solution was unstable at room temperature or lower and spontaneously formed an opaque gel within a few of hours due to the crystallization of PCL segments. In addition, the crystallization of PCL blocks led to a very low degradation rate of the hydrogel in vivo, as displayed in Figure 5. The incorporation of GA segments effectively hindered the regular crystallization of PCL blocks as evidenced by DSC and XRD analysis (Figure 2). In the case of P3 with a high GA content, neither the melting/crystallization peak in DSC nor the diffraction peak in XRD was observed, indicating that the polymer lost the ability of crystallization and just exhibited an amorphous state. As a result, bulk P3 just showed a sticky paste, resulting in the difficulty in handling, weighing, and transferring. P2 copolymer not only kept a powder form in bulk but also exhibited a stable solution state after dissolution in water (Figure 3), which was convenient to handle and store. This feature was attributed to an adequate crystallization ability of the triblock copolymer achieved by the appropriate CL-to-GA ratio. Meanwhile, the degradation of these polymer hydrogels mainly depends on the hydrolysis of polyester segments, and the introduction of GA units significantly accelerated the degradation of hydrogels in vivo due to both the destruction of crystallization of PCL blocks and the higher hydrolysis rate of GA segments.<sup>52</sup> Consequently, the in vivo persistence time of P2 gel reduced to 3–4 weeks, while the in vivo integrity of P3 system was not more than 3 weeks (Figure 5). Their final degradation fragments are glycolic acid, 1,6-hydroxycaproic acid, and nondegradable PEG, which are nontoxic and easily cleared from body.<sup>45,46,53,54</sup>

#### Convenient Loading and Sustained Release of Drugs.

All of the polymer/water systems underwent sol–gel transitions as the temperature increased and formed nonflowing physical hydrogels at body temperature (Figure 4), indicating that they can be used as minimally invasive injectable carriers for sustained drug delivery. Meanwhile, the feature of sol–gel transition enabled convenient encapsulation of Lira at low temperature without any loss, and this process was free of any organic solvent. These advantages were beneficial in avoiding the degradation or denaturation of loaded Lira.

In vitro release tests demonstrated that all the Lira-loaded gel formulations exhibited a relatively slow and consistent release rate of drug during the 10 day examination period, and no significant difference among them was observed (Figure 7). The similar release profiles revealed that the introduction of GA

into PCL block had no significant influence on the drug release behavior. Furthermore, we confirmed that diffusion-controlled mechanism governed the release of Lira from the hydrogel depots. Such a sustained drug release manner was attributed to the hydrophobic interaction of the drug and carrier polymers due to the amphiphilic nature of both Lira polypeptide and polyester-PEG-polyester copolymers, or, to be more precise, the hydrophobic interaction between C16 side chain of Lira and polyester segments of carrier polymers resulted in the sustained release of drug from the hydrogel matrix. In contrast, hydrophilic polypeptides, such as insulin and exenatide, just displayed a high burst effect and a short release duration from the similar thermosensitive hydrogels owing to absence of such a hydrophobic interaction between drugs and carriers.<sup>47,50,55</sup> It is worth pointing out that this question is still open, and thus, further studies are needed to provide more direct evidence. In addition, dynamic rheological measurement demonstrated that the introduction of Lira into P2 aqueous solution had no obvious influence on the sol-gel transition temperature of hydrogel system and its injectability yet resulted in a certain degree of increase in both storage modulus  $G'$  and complex viscosity  $\eta$  of the hydrogel formulation, as displayed in Figure S3.

Taken together with the convenience of administration of carrier polymers and the *in vivo* integrity maintenance of gels, we finally selected P2 copolymer as the optimal carrier polymer to perform the *in vivo* evaluation while minimizing the number of animals used. Lira was labeled by Cy5.5 fluorescent dye and then loaded into P2 gel to noninvasively track the *in vivo* release of drug from the optimal Lira formulation. The *in vivo* imaging in mice showed that the sustained release of drug from P2 gel lasted for more than 10 days (Figure 8), which was coincidence with the *in vitro* release profile.

**Long-Term Glycemic Control, Effective Body Weight Reduction, and Enhanced Pancreatic Function.** The mutant mouse, C57BLKS/J db/db, is able to develop spontaneously diabetes, and its phenotypes are similar to those of T2DM patients.<sup>56</sup> Thus, we choose this animal model for the *in vivo* evaluation of hypoglycemic efficacy. After a single administration in diabetic db/db mice, the Lira-loaded P2 gel formulation achieved a week-long glycemic control in normal levels (Figure 9). Subsequently, the blood glucose of mice in the Lira/Gel group gradually rebounded to the high level, but it was still significantly lower than that of the blank gel group on day 10 postinjection. These features were consistent with both the *in vitro* release profile and the *in vivo* imaging results and attributed to the continuous liberation of drug from the gel by diffusion. The change in body weight of mice over time was also recorded (Figure 10). The moderate reduction of body weight in db/db mice was achieved by the administration of Lira solution or the gel formulation, which was very helpful for the T2DM patients with obesity. In fact, the once-daily injection of Lira (Saxenda) has been approved by FDA in 2014 for body-weight management.<sup>57</sup> Therefore, our Lira-loaded gel formulation may also serve as a promising long-acting formulation for antiobesity. Moreover, the sustained *in vivo* hypoglycemic efficacy and effective body weight reduction further confirmed that released Lira was bioactive and did not suffer from the degradation or denaturation in the gel matrix.

HbA<sub>1c</sub> comes from irreversible glycation of hemoglobin and is not influenced by temporary blood glucose fluctuation. Thus, it has been acknowledged as a golden standard for monitoring of average glycemic control over the previous several months.<sup>58</sup>

Considering that the interval of reliable detection of HbA<sub>1c</sub> usually requires at least one month in humans, we prolonged the experimental duration to 30 days through successive administrations of two more gel formulations to mice. The results showed that the HbA<sub>1c</sub> levels in both the groups of Lira solution and Lira/Gel were significantly lower than that of the blank gel group, inflecting the efficient glycemic control of mice within the one-month experimental period. Meanwhile, there was no significant difference of HbA<sub>1c</sub> between the two treatment groups (Figure 11). These findings indicate that our long-acting formulation can achieve a comparable long-term glycemic control with once-daily administration of Lira solution, whereas it is more convenient for patients with greatly reduced frequency of injection.

It is well-known that  $\beta$ -cell function progressively deteriorates in patients with T2DM.<sup>59</sup> Therefore, it is very important to preserve  $\beta$ -cell function in pancreatic islets in treatment of T2DM. We performed histological observations to evaluate the  $\beta$ -cell function after administration of our Lira formulation for one month (Figure 12). The results of histological examinations showed that the treatment of Lira-loaded gel formulation not only promoted the proliferation of islet cells but also improved the  $\beta$ -cell function in db/db mice. This feature coincides well with the pharmacology of Lira as reviewed in the previous literature.<sup>11,13</sup>

## 5. CONCLUSIONS

In this study, we successfully developed an expected once-weekly injectable hydrogel formulation of Lira. A total of three thermosensitive PCGA-PEG-PCGA triblock copolymers with different CL-to-GA ratios were designed and synthesized. The PCGA-PEG-PCGA copolymer with a CL-to-GA ratio of 5:1 exhibited a powder form in bulk and maintained a stable aqueous solution before heating, which is easy to handle and store. Meanwhile, the proper degradation rate *in vivo* of this gel is able to meet with the requirement of repeated administrations in treatment of T2DM patients. A single injection of such an optimal Lira-loaded hydrogel formulation showed a remarkably hypoglycemic efficacy, up to 1 week in diabetic db/db mice. Furthermore, multiple administrations of this formulation significantly lowered HbA<sub>1c</sub> and protected islets of db/db mice. Hence, a once-weekly injectable hydrogel formulation of antidiabetic liraglutide with great improvement of patient compliance was achieved, and this formulation has great potential for repeated administrations in T2DM patients in a long-term glycemic control.

## ■ ASSOCIATED CONTENT

### Supporting Information

The Supporting Information is available free of charge on the ACS Publications website at DOI: 10.1021/acsami.6b09415

<sup>1</sup>H NMR spectra and GPC chromatograms of copolymers, rheological studies of the copolymer aqueous solutions, thermal properties of the copolymers measured by DSC, and *in vitro* release kinetic assessment. (PDF).

## ■ AUTHOR INFORMATION

### Corresponding Author

\*E-mail: [yu\\_lin@fudan.edu.cn](mailto:yu_lin@fudan.edu.cn); tel.: +86 021 65642531; fax: +86 021 65640293.

## Author Contributions

The manuscript was written through contributions of all authors. All authors have given approval to the final version of the manuscript.

## Notes

The authors declare no competing financial interest.

## ACKNOWLEDGMENTS

The authors are grateful for the financial support from National Natural Science Foundation of China (grant nos. 21474019 and 51273217), Chinese Ministry of Science and Technology (863 program no. 2015AA033703), State Key Project of Research and Development (grant no. 2016YFC1100300), Science and Technology Developing Foundation of Shanghai (grant nos. 15JC1490300 and 14441901500).

## REFERENCES

- (1) Russell-Jones, D.; Gough, S. Recent Advances in Incretin-Based Therapies. *Clin. Endocrinol.* **2012**, *77*, 489–499.
- (2) Tahrani, A. A.; Piya, M. K.; Kennedy, A.; Barnett, A. H. Glycaemic Control in Type 2 Diabetes: Targets and New Therapies. *Pharmacol. Ther.* **2010**, *125*, 328–361.
- (3) Kim, H.; Park, H.; Lee, J.; Kim, T. H.; Lee, E. S.; Oh, K. T.; Lee, K. C.; Youn, Y. S. Highly Porous Large Poly(Lactic-co-Glycolic Acid) Microspheres Adsorbed with Palmityl-Acylated Exendin-4 as a Long-Acting Inhalation System for Treating Diabetes. *Biomaterials* **2011**, *32*, 1685–1693.
- (4) Doyle, M. E.; Egan, J. M. Mechanisms of Action of Glucagon-Like Peptide 1 in the Pancreas. *Pharmacol. Ther.* **2007**, *113*, 546–593.
- (5) Baggio, L. L.; Drucker, D. J. Biology of Incretins: GLP-1 and GIP. *Gastroenterology* **2007**, *132*, 2131–2157.
- (6) Deacon, C. F. Therapeutic Strategies Based on Glucagon-Like Peptide 1. *Diabetes* **2004**, *53*, 2181–2189.
- (7) Nauck, M. A.; Meier, J. J. Glucagon-Like Peptide 1 and Its Derivatives in the Treatment of Diabetes. *Regul. Pept.* **2005**, *128*, 135–148.
- (8) Montanya, E.; Sesti, G. A Review of Efficacy and Safety Data Regarding the Use of Liraglutide, a Once-Daily Human Glucagon-Like Peptide 1 Analogue, in the Treatment of Type 2 Diabetes Mellitus. *Clin. Ther.* **2009**, *31*, 2472–2488.
- (9) Vilsboll, T. Liraglutide: A Once-Daily GLP-1 Analogue for the Treatment of Type 2 Diabetes Mellitus. *Expert Opin. Invest. Drugs* **2007**, *16*, 231–237.
- (10) Ryan, G. J.; Foster, K. T.; Jobe, L. J. Review of the Therapeutic Uses of Liraglutide. *Clin. Ther.* **2011**, *33*, 793–811.
- (11) Vilsboll, T.; Brock, B.; Perrild, H.; Levin, K.; Lervang, H. H.; Kolendorf, K.; Krarup, T.; Schmitz, O.; Zdravkovic, M.; Le-Thi, T.; Madsbad, S. Liraglutide, a Once-Daily Human GLP-1 Analogue, Improves Pancreatic  $\beta$ -Cell Function and Arginine-Stimulated Insulin Secretion During Hyperglycaemia in Patients with Type 2 Diabetes Mellitus. *Diabetic Med.* **2008**, *25*, 152–156.
- (12) Raun, K.; von Voss, P.; Gotfredsen, C. F.; Golozoubova, V.; Rolin, B.; Knudsen, L. B. Liraglutide, a Long-Acting Glucagon-Like Peptide-1 Analog, Reduces Body Weight and Food Intake in Obese Candy-Fed Rats, Whereas a Dipeptidyl Peptidase-IV Inhibitor, Vildagliptin, Does Not. *Diabetes* **2007**, *56*, 8–15.
- (13) Mari, A.; Degen, K.; Brock, B.; Rungby, J.; Ferrannini, E.; Schmitz, O. Effects of the Long-Acting Human Glucagon-Like Peptide-1 Analog Liraglutide on  $\beta$ -Cell Function in Normal Living Conditions. *Diabetes Care* **2007**, *30*, 2032–2033.
- (14) Vilsboll, T.; Zdravkovic, M.; Le-Thi, T.; Krarup, T.; Schmitz, O.; Courreges, J. P.; Verhoeven, R.; Buganova, I.; Madsbad, S. Liraglutide, a Long-Acting Human Glucagon-Like Peptide-1 Analog, Given as Monotherapy Significantly Improves Glycemic Control and Lowers Body Weight without Risk of Hypoglycemia in Patients with Type 2 Diabetes. *Diabetes Care* **2007**, *30*, 1608–1610.
- (15) Vermonden, T.; Censi, R.; Hennink, W. E. Hydrogels for Protein Delivery. *Chem. Rev.* **2012**, *112*, 2853–2888.
- (16) Petit, A.; Sandker, M.; Muller, B.; Meyboom, R.; van Midwoud, P.; Bruin, P.; Redout, E. M.; Versluis-Helder, M.; van der Lest, C. H. A.; Buwalda, S. J.; de Leede, L. G. J.; Vermonden, T.; Kok, R. J.; Weinans, H.; Hennink, W. E. Release Behavior and Intra-Articular Biocompatibility of Celecoxib-Loaded Acetyl-Capped PCLA-PEG-PCLA Thermogels. *Biomaterials* **2014**, *35*, 7919–7928.
- (17) Nikouei, N. S.; Ghasemi, N.; Lavasanifar, A. Temperature/pH Responsive Hydrogels Based on Poly(Ethylene Glycol) and Functionalized Poly( $\epsilon$ -Caprolactone) Block Copolymers for Controlled Delivery of Macromolecules. *Pharm. Res.* **2016**, *33*, 358–366.
- (18) Wu, D. Q.; Qiu, F.; Wang, T.; Jiang, X. J.; Zhang, X. Z.; Zhuo, R. X. Toward the Development of Partially Biodegradable and Injectable Thermoresponsive Hydrogels for Potential Biomedical Applications. *ACS Appl. Mater. Interfaces* **2009**, *1*, 319–327.
- (19) Lee, C.; Choi, J. S.; Kim, I.; Byeon, H. J.; Kim, T. H.; Oh, K. T.; Lee, E. S.; Lee, K. C.; Youn, Y. S. Decanoic Acid-Modified Glycol Chitosan Hydrogels Containing Tightly Adsorbed Palmityl-Acylated Exendin-4 as a Long-Acting Sustained-Release Anti-Diabetic System. *Acta Biomater.* **2014**, *10*, 812–820.
- (20) Ma, H. C.; He, C. L.; Cheng, Y. L.; Yang, Z. M.; Zang, J. T.; Liu, J. G.; Chen, X. S. Localized Co-Delivery of Doxorubicin, Cisplatin, and Methotrexate by Thermosensitive Hydrogels for Enhanced Osteosarcoma Treatment. *ACS Appl. Mater. Interfaces* **2015**, *7*, 27040–27048.
- (21) Park, M. H.; Joo, M. K.; Choi, B. G.; Jeong, B. Biodegradable Thermogels. *Acc. Chem. Res.* **2012**, *45*, 424–433.
- (22) Wang, Z. C.; Xu, X. D.; Chen, C. S.; Yun, L.; Song, J. C.; Zhang, X. Z.; Zhuo, R. X. In Situ Formation of Thermosensitive PNIPAAm-Based Hydrogels by Michael-Type Addition Reaction. *ACS Appl. Mater. Interfaces* **2010**, *2*, 1009–1018.
- (23) Huang, C. C.; Liao, Z. X.; Chen, D. Y.; Hsiao, C. W.; Chang, Y.; Sung, H. W. Injectable Cell Constructs Fabricated via Culture on a Thermoresponsive Methylcellulose Hydrogel System for the Treatment of Ischemic Diseases. *Adv. Healthcare Mater.* **2014**, *3*, 1133–1148.
- (24) Dong, X.; Wei, C.; Liu, T. J.; Lv, F.; Qian, Z. Y. Real-Time Fluorescence Tracking of Protoporphyrin Incorporated Thermosensitive Hydrogel and Its Drug Release in Vivo. *ACS Appl. Mater. Interfaces* **2016**, *8*, 5104–5113.
- (25) Shen, W. J.; Luan, J. B.; Cao, L. P.; Sun, J.; Yu, L.; Ding, J. D. Thermogelling Polymer-Platinum(IV) Conjugates for Long-Term Delivery of Cisplatin. *Biomacromolecules* **2015**, *16*, 105–115.
- (26) Nikouei, N. S.; Vakili, M. R.; Bahniuk, M. S.; Unsworth, L.; Akbari, A.; Wu, J. P.; Lavasanifar, A. Thermoreversible Hydrogels Based on Triblock Copolymers of Poly(Ethylene Glycol) and Carboxyl Functionalized Poly( $\epsilon$ -Caprolactone): The Effect of Carboxyl Group Substitution on the Transition Temperature and Biocompatibility in Plasma. *Acta Biomater.* **2015**, *12*, 81–92.
- (27) Li, X. Z.; Ding, J. X.; Zhang, Z. Z.; Yang, M. D.; Yu, J. K.; Wang, J. C.; Chang, F.; Chen, X. S. Kartogenin-Incorporated Thermogel Supports Stem Cells for Significant Cartilage Regeneration. *ACS Appl. Mater. Interfaces* **2016**, *8*, 5148–5159.
- (28) Ci, T. Y.; Chen, L.; Yu, L.; Ding, J. D. Tumor Regression Achieved by Encapsulating a Moderately Soluble Drug into a Polymeric Thermogel. *Sci. Rep.* **2014**, *4*, 5473.
- (29) Kim, S.-J.; Park, M. H.; Moon, H. J.; Park, J. H.; Ko, D. Y.; Jeong, B. Polypeptide Thermogels as a Three Dimensional Culture Scaffold for Hepatogenic Differentiation of Human Tonsil-Derived Mesenchymal Stem Cells. *ACS Appl. Mater. Interfaces* **2014**, *6*, 17034–17043.
- (30) Patel, M.; Moon, H. J.; Ko, D. Y.; Jeong, B. Composite System of Graphene Oxide and Polypeptide Thermogel as an Injectable 3d Scaffold for Adipogenic Differentiation of Tonsil-Derived Mesenchymal Stem Cells. *ACS Appl. Mater. Interfaces* **2016**, *8*, 5160–5169.
- (31) Seo, B. B.; Choi, H.; Koh, J. T.; Song, S. C. Sustained BMP-2 Delivery and Injectable Bone Regeneration Using Thermosensitive

Polymeric Nanoparticle Hydrogel Bearing Dual Interactions with BMP-2. *J. Controlled Release* **2015**, *209*, 67–76.

(32) Park, M. R.; Chun, C. J.; Ahn, S. W.; Ki, M. H.; Cho, C. S.; Song, S. C. Sustained Delivery of Human Growth Hormone Using a Polyelectrolyte Complex-Loaded Thermosensitive Polyphosphazene Hydrogel. *J. Controlled Release* **2010**, *147*, 359–367.

(33) Boffito, M.; Sirianni, P.; Di Rienzo, A. M.; Chiono, V. Thermosensitive Block Copolymer Hydrogels Based on Poly( $\epsilon$ -Caprolactone) and Polyethylene Glycol for Biomedical Applications: State of the Art and Future Perspectives. *J. Biomed. Mater. Res., Part A* **2015**, *103*, 1276–1290.

(34) Nguyen, M. K.; Lee, D. S. Injectable Biodegradable Hydrogels. *Macromol. Biosci.* **2010**, *10*, 563–579.

(35) Chen, L.; Ci, T. Y.; Yu, L.; Ding, J. D. Effects of Molecular Weight and Its Distribution of Peg Block on Micellization and Thermogellability of PLGA-PEG-PLGA Copolymer Aqueous Solutions. *Macromolecules* **2015**, *48*, 3662–3671.

(36) Yu, L.; Hu, H. T.; Chen, L.; Bao, X. G.; Li, Y. Z.; Xu, G. H.; Ye, X. J.; Ding, J. D.; Chen, L. Comparative Studies of Thermogels in Preventing Post-Operative Adhesions and Corresponding Mechanisms. *Biomater. Sci.* **2014**, *2*, 1100–1109.

(37) Yu, L.; Sheng, W. J.; Yang, D. C.; Ding, J. D. Design of Molecular Parameters to Achieve Block Copolymers with a Powder Form at Dry State and a Temperature-Induced Sol-Gel Transition in Water without Unexpected Gelling Prior to Heating. *Macromol. Res.* **2013**, *21*, 207–215.

(38) Cao, L. P.; Cao, B.; Lu, C. J.; Wang, G. W.; Yu, L.; Ding, J. D. An Injectable Hydrogel Formed by In Situ Cross-Linking of Glycol Chitosan and Multi-Benzaldehyde Functionalized PEG Analogues for Cartilage Tissue Engineering. *J. Mater. Chem. B* **2015**, *3*, 1268–1280.

(39) Yeo, J.; Kang, Y. J.; Jeon, S. M.; Jung, U. J.; Lee, M. K.; Song, H.; Choi, M. S. Potential Hypoglycemic Effect of an Ethanol Extract of *Gynostemma pentaphyllum* in C57BL/KsJ-db/db Mice. *J. Med. Food* **2008**, *11*, 709–716.

(40) Moon, H.; Chon, J.; Joo, J.; Kim, D.; In, J.; Lee, H.; Park, J.; Choi, J. FTY720 Preserved Islet  $\beta$ -Cell Mass by Inhibiting Apoptosis and Increasing Survival of  $\beta$ -Cells in db/db Mice. *Diabetes/Metab. Res. Rev.* **2013**, *29*, 19–24.

(41) Bae, S. J.; Suh, J. M.; Sohn, Y. S.; Bae, Y. H.; Kim, S. W.; Jeong, B. Thermogelling Poly(Caprolactone-*b*-Ethylene Glycol-*b*-Caprolactone) Aqueous Solutions. *Macromolecules* **2005**, *38*, 5260–5265.

(42) Gong, C. Y.; Shi, S. A.; Wu, L.; Gou, M. L.; Yin, Q. Q.; Guo, Q. F.; Dong, P. W.; Zhang, F.; Luo, F.; Zhao, X.; Wei, Y. Q.; Qian, Z. Y. Biodegradable in Situ Gel-Forming Controlled Drug Delivery System Based on Thermosensitive PCL-PEG-PCL Hydrogel. Part 2: Sol-Gel-Sol Transition and Drug Delivery Behavior. *Acta Biomater.* **2009**, *5*, 3358–3370.

(43) Jiang, Z. Q.; You, Y. J.; Deng, X. M.; Hao, J. Y. Injectable Hydrogels of Poly( $\epsilon$ -Caprolactone-co-Glycolide)-Poly(Ethylene Glycol)-Poly( $\epsilon$ -Caprolactone-co-Glycolide) Triblock Copolymer Aqueous Solutions. *Polymer* **2007**, *48*, 4786–4792.

(44) Yu, L.; Zhang, Z.; Zhang, H.; Ding, J. D. Biodegradability and Biocompatibility of Thermoreversible Hydrogels Formed from Mixing a Sol and a Precipitate of Block Copolymers in Water. *Biomacromolecules* **2010**, *11*, 2169–2178.

(45) Zentner, G. M.; Rath, R.; Shih, C.; McRea, J. C.; Seo, M. H.; Oh, H.; Rhee, B. G.; Mestecky, J.; Moldoveanu, Z.; Morgan, M.; Weitman, S. Biodegradable Block Copolymers for Delivery of Proteins and Water-Insoluble Drugs. *J. Controlled Release* **2001**, *72*, 203–215.

(46) Kang, Y. M.; Lee, S. H.; Lee, J. Y.; Son, J. S.; Kim, B. S.; Lee, B.; Chun, H. J.; Min, B. H.; Kim, J. H.; Kim, M. S. A Biodegradable, Injectable, Gel System Based on MPEG-*b*-(PCL-*ran*-PLLA) Diblock Copolymers with an Adjustable Therapeutic Window. *Biomaterials* **2010**, *31*, 2453–2460.

(47) Li, K.; Yu, L.; Liu, X. J.; Chen, C.; Chen, Q. H.; Ding, J. D. A Long-Acting Formulation of a Polypeptide Drug Exenatide in Treatment of Diabetes Using an Injectable Block Copolymer Hydrogel. *Biomaterials* **2013**, *34*, 2834–2842.

(48) Malm-Erfjelt, M.; Bjornsdottir, I.; Vanggaard, J.; Helleberg, H.; Larsen, U.; Oosterhuis, B.; van Lier, J. J.; Zdravkovic, M.; Olsen, A. K. Metabolism and Excretion of the Once-Daily Human Glucagon-Like Peptide-1 Analog Liraglutide in Healthy Male Subjects and Its In Vitro Degradation by Dipeptidyl Peptidase IV and Neutral Endopeptidase. *Drug Metab. Dispos.* **2010**, *38*, 1944–1953.

(49) Kwak, H. H.; Shim, W. S.; Hwang, S.; Son, M. K.; Kim, Y. J.; Kim, T. H.; Yoon, Z. H.; Youn, H. J.; Lee, G. I.; Kang, S. H.; Shim, C. K. Pharmacokinetics and Efficacy of a Biweekly Dosage Formulation of Exenatide in Zucker Diabetic Fatty (ZDF) Rats. *Pharm. Res.* **2009**, *26*, 2504–2512.

(50) Choi, S.; Kim, S. W. Controlled Release of Insulin from Injectable Biodegradable Triblock Copolymer Depot in ZDF Rats. *Pharm. Res.* **2003**, *20*, 2008–2010.

(51) Chen, S.; Singh, J. Controlled Release of Growth Hormone from Thermosensitive Triblock Copolymer Systems: In Vitro and In Vivo Evaluation. *Int. J. Pharm.* **2008**, *352*, 58–65.

(52) Yu, L.; Zhang, Z.; Ding, J. D. In Vitro Degradation and Protein Release of Transparent and Opaque Physical Hydrogels of Block Copolymers at Body Temperature. *Macromol. Res.* **2012**, *20*, 234–243.

(53) Zhang, Z.; Ni, J.; Chen, L.; Yu, L.; Xu, J. W.; Ding, J. D. Biodegradable and Thermoreversible PCLA-PEG-PCLA Hydrogel as a Barrier for Prevention of Post-Operative Adhesion. *Biomaterials* **2011**, *32*, 4725–4736.

(54) Petit, A.; Muller, B.; Meijboom, R.; Bruin, P.; van de Manakker, F.; Versluis-Helder, M.; de Leede, L. G. J.; Doornbos, A.; Landin, M.; Hennink, W. E.; Vermonden, T. Effect of Polymer Composition on Rheological and Degradation Properties of Temperature-Responsive Gelling Systems Composed of Acyl-Capped PCLA-PEG-PCLA. *Biomacromolecules* **2013**, *14*, 3172–3182.

(55) Huynh, D. P.; Nguyen, M. K.; Pi, B. S.; Kim, M. S.; Chae, S. Y.; Kang, C. L.; Bong, S. K.; Kim, S. W.; Lee, D. S. Functionalized Injectable Hydrogels for Controlled Insulin Delivery. *Biomaterials* **2008**, *29*, 2527–2534.

(56) Coleman, D. L.; Hummel, K. P. Studies with the Mutation, Diabetes, in the Mouse. *Diabetologia* **1967**, *3*, 238–248.

(57) Nuffer, W. A.; Trujillo, J. M. Liraglutide: A New Option for the Treatment of Obesity. *Pharmacotherapy* **2015**, *35*, 926–934.

(58) Krishnamurti, U.; Steffes, M. W. Glycohemoglobin: A Primary Predictor of the Development or Reversal of Complications of Diabetes Mellitus. *Clin. Chem.* **2001**, *47*, 1157–1165.

(59) Butler, A. E.; Janson, J.; Bonner-Weir, S.; Ritzel, R.; Rizza, R. A.; Butler, P. C.  $\beta$ -Cell Deficit and Increased  $\beta$ -Cell Apoptosis in Humans with Type 2 Diabetes. *Diabetes* **2003**, *52*, 102–110.